Plant Physiology and Biochemistry 118 (2017) 88–97

Contents lists available at ScienceDirect

Plant Physiology and Biochemistry

journal homepage: www.elsevier.com/locate/plaphy

Research article

Photoprotection regulated by phosphorus application can improve photosynthetic performance and alleviate oxidative damage in dwarf bamboo subjected to water stress

Chenggang Liu [a, b], Yanjie Wang [c, *], Yanqiang Jin [a], Kaiwen Pan [a], Xingmei Zhou [a], Na Li [a]

[a] Key Laboratory of Mountain Ecological Restoration and Bioresource Utilization & Ecological Restoration Biodiversity Conservation Key Laboratory of Sichuan Province, Chengdu Institute of Biology, Chinese Academy of Sciences, Chengdu 610041, China
[b] Key Laboratory of Tropical Plant Resources and Sustainable Use, Xishuangbanna Tropical Botanical Garden, Chinese Academy of Sciences, Menglun 666303, China
[c] College of Life Science, Sichuan Normal University, Chengdu 610101, China

ARTICLE INFO

Article history:
Received 1 April 2017
Received in revised form
30 May 2017
Accepted 31 May 2017
Available online 8 June 2017

Keywords:
Phosphorus addition
Ascorbate
Electron transport capacity
Xanthophyll cycle
Thermal dissipation
Oxidative stress

ABSTRACT

Water and nutrients, particularly phosphorus (P), are the two most limiting factors for dwarf bamboo growth in tropical and subtropical areas. Dwarf bamboo is highly sensitive to water stress and often causes severe P deficiency in its growing soils due to the characteristics of shallower roots and expeditious growth. However, little is known about its photoprotective response to soil water deficit and the underlying mechanisms regulated by P application. In this study, a completely randomized design with two factors of two water regimes (well-watered and water-stressed) and two P levels (with and without P application) was arranged to investigate this issue in dwarf bamboo (*Fargesia rufa*) plants. Water stress not only decreased water status and photochemical activity but also increased lipid peroxidation due to reactive oxygen species (ROS) accumulation irrespective of P application. In this case, thermal dissipation and antioxidative defense were promoted. Moreover, the role of the water–water cycle under this stress still could not be ignored because it accounted for a large proportion of total energy (J_{PSII}). P application significantly enhanced photochemical activity accompanied by increased chlorophyll content in water-stressed plants. Meanwhile, P application remarkably reduced thermal dissipation and hardly affected photorespiration and the water–water cycle under water stress. Although P application only enhanced ascorbate (AsA) level, ROS, particularly hydrogen peroxide (H_2O_2), and lipid peroxidation were significantly reduced in water-stressed plants. Therefore, P application can improve the photosynthetic capacity by regulating the redistribution of energy absorbed by PSII antennae and independently activating of the H_2O_2-scavenging function of AsA to alleviate oxidative damage in *F. rufa* plants, thereby improving their survival under water stress conditions.

1. Introduction

Water and nutrients are two of the most critical factors affecting plant growth and productivity, and they are closely related with each other (Graciano et al., 2006; Simancas et al., 2016). However, their relative importance may vary for soil properties and climatic conditions, such as rainfall (Graciano et al., 2005). Several studies have suggested that irrigation is highly effective in nutrient-rich

Abbreviations: APX, ascorbate peroxidase; AsA, reduced ascorbate; C_i, intercellular CO_2 concentration; DEPS, de-epoxidation state of xanthophyll cycle; DHA, oxidized ascorbate; DHAR, dehydroascorbate reductase; F_v/F_m, maximum quantum efficiency of PSII; GR, glutathione reductase; g_s, stomatal conductance; GSH, reduced glutathione; GSSG, oxidized glutathione; H_2O_2, hydrogen peroxide; $J_{f,D}$, energy flux *via* fluorescence and constitutive thermal dissipation; J_{NPQ}, energy flux *via* △pH- and xanthophyll-regulated thermal dissipation; J_{PSII}, energy flux *via* linear electron transport in PSII; $J_a(O_2\text{-dependent})$, O_2-dependent alternative electron flux; $J_a(O_2\text{-independent})$, O_2-independent alternative electron flux; J_{PCO}, electron flux for photorespiratory carbon oxidation; J_{PCR}, electron flux for photosynthetic carbon reduction; LRWC, leaf relative water content; MDA, malondialdehyde; MDHAR, monodehydroascorbate reductase; NPQ, thermal dissipation efficiency; $O_2^{\bullet-}$, superoxide anion; P_n, CO_2 assimilation rate; ROS, reactive oxygen species; SOD, superoxide dismutase; tAsA, total ascorbate; tGSH, total glutathione; VAZ, xanthophyll cycle pool; Φ_{PSII}, quantum yield of PSII electron transport.

* Corresponding author.
E-mail address: wyjilwm2015@163.com (Y. Wang).

http://dx.doi.org/10.1016/j.plaphy.2017.05.022
0981-9428/

soils, and that fertilization is highly effective in soils without water stress (Suriyagoda et al., 2014; Eskelinen and Harrison, 2015). Consequently, rational application of fertilizers with irrigation has become a key measure to improve plant productivity in sustainable agriculture and forestry systems. Moreover, improperly using water and fertilizers can not only cause resource wastage and environmental damage but also result in ecological stresses on plant growth and survival (Yin et al., 2012).

Changes in water and nutrient availability can elicit common and specific plant responses, including morphological and physiobiochemical alterations at the subcellular, cellular, and whole-plant levels (Kudoyarova et al., 2015). Water and nutrient deficiencies in soils inhibit photosynthesis through stomatal closure and/or metabolic impairment and cause light energy absorption to exceed its utilization, thereby resulting in photoinhibition and photooxidative stress to the photosynthetic apparatus due to overproduction of reactive oxygen species (ROS), such as superoxide anion ($O_2^{\bullet-}$) and hydrogen peroxide (H_2O_2) (Adams et al., 2013; Cortina et al., 2013; Singh et al., 2016). Accordingly, a plethora of photoprotective mechanisms counterbalancing the use of absorbed energy for photosynthesis and the safe dissipation methods of excess energy, such as thermal dissipation, photorespiration, and the water–water cycle, can be important in circumventing the potential damaging (Gallé et al., 2007; Liu et al., 2017a). In addition to chloroplasts, mitochondria are also ROS-producing sites because they consume up to 2% of the total O_2 evolved by chloroplasts to form ROS mainly through Complexes I and III in the mitochondrial electron transport chain (Das and Roychoudhury, 2014). Moreover, cytosol is considered to be an essential sink for ROS generated in other organelles (Hu et al., 2005). Excessive ROS formation in different organelles will induce oxidative damage that is usually characterized by increased lipid peroxidation level (Noctor and Foyer, 2016). Meanwhile, these organelles have a complex battery of antioxidative systems, including enzymes, such as superoxide dismutase (SOD), and those involved in the ascorbate-glutathione cycle; as well as non-enzymatic antioxidants, such as ascorbate, glutathione, and carotenoids, to control ROS levels and prevent or minimize lipid peroxidation (Wujeska et al., 2013; Noctor and Foyer, 2016). Hence, isolated organelles are often used to study the capacity of their respective antioxidative system response to stresses.

Phosphorus (P) is required for many aspects of plant physiology, such as photosynthetic energy processes and carbohydrate transport (Gan et al., 2016; Simancas et al., 2016). However, more than 80% of P provided as fertilizers in soil can be fixed in unavailable forms for plants. Moreover, the concentrations of orthophosphate (P_i) forms (HPO_4^{2-} and $H_2PO_4^-$) most readily absorbed by roots are very low and rarely exceed 10 μM in soil solutions (Hernández and Munné-Bosch, 2015). Therefore, P is second only to nitrogen as the most limiting nutrient for plant productivity. In particular, under water stress, P availability in soils will become low due to the decline of water availability, thereby leading to a significant loss in productivity (Suriyagoda et al., 2014). To ensure plant productivity, applying P to the soil is necessary. Several studies indicated that P application can enhance drought tolerance of plants through a series of structural, physiological, and biochemical changes, such as more dry matter allocation to leaves than roots, increase of xylem hydraulic conductivity and water use efficiency, enhancement of photosynthetic capacity, and acceleration in nitrate assimilation during water stress (Singh and Sale, 2000; dos Santos et al., 2004; Jones et al., 2005; Burman et al., 2009; Cortina et al., 2013; Kuwahara et al., 2016). However, these knowledge of the response of water-stressed plants to P application is based mainly on woody and herbaceous plants, which have P nutrition strategies that are distinct from those of semi-woody plants. For instance, our previous study showed that P application slows nitrogen metabolism in water-stressed dwarf bamboo (Liu et al., 2015a). Importantly, limited information is available regarding the impact of P application on different photoprotective mechanisms (Morales et al., 2006; Simancas et al., 2016), particularly semi-woody plants during acclimation to water stress.

Dwarf bamboo, as semi-woody plant, belongs to rhizomatous perennial species and is widely distributed in subtropical and tropical areas. Moreover, dwarf bamboo has shallow roots and grows expeditiously, making it highly sensitive to water stress and causing severe P deficiency in its growing soils (Divakara et al., 2001; Chen et al., 2011). This condition impedes natural regeneration of seedlings in its dominated forests and decreases ecosystem productivity. However, only few studies have been conducted on the responses of dwarf bamboo to different environmental stresses (Li et al., 2013; Liu et al., 2015b, 2017a, b) and the underlying regulation mechanisms after mineral nutrient (e.g., P) application under such conditions (Liu et al., 2015a).

Therefore, in the present study, dwarf bamboo (*Fargesia rufa* Yi), one of the staple foods of the endangered giant pandas, was used to investigate how P application regulates various photoprotective pathways of this species exposed to water stress. We hypothesized that P application would enhance *F. rufa* resistance to water stress by upregulating different photoprotective pathways against oxidative damage. To verify this hypothesis, gas exchange and chlorophyll (Chl) *a* fluorescence parameters were measured to estimate the allocation of photosynthetic electron fluxes. Simultaneously, the activities of key antioxidative enzymes at the organelle level and the contents of some important antioxidants were quantified to analyze ROS scavenging capacity. Furthermore, water status of leaves, pigments content, ROS generation, and lipid peroxidation were determined.

2. Materials and methods

2.1. Plant material and experimental setup

The experiment was conducted at Maoxian Ecological Station of Chinese Academy of Sciences (103°53′E, 31°41′N, 1826 m a.s.l.) in Southwestern China. Two-year-old uniform and healthy *F. rufa* plants (40 ± 5 cm in height) were obtained from the nursery at Wanglang National Nature Reserve. The plants were transplanted separately into 50 l plastic pots filled with 25 kg of homogenized and sieved surface soil (0–30 cm) from the experimental site, moved into a semi-controlled environment greenhouse with a temperature range of 15 °C–33 °C and a relative humidity of 50%–80%, and watered regularly with water from a nearby stream. Each pot had one standard plant with 4–5 ramets. Furthermore, organic matter content (14.02 g kg^{-1}), total P (0.67 g kg^{-1}), and available P (5.10 mg kg^{-1}) in soil were first measured before the experiment.

Approximately four months after transplanting, the experimental treatments were initiated and continued until the end of study (45 days). The experiment was arranged in a randomized complete block design with two factors of two water regimes and two P fertilization levels. First, the two P fertilization treatments were implemented: without P application [no application of P fertilizer to each pot (−P)] and with P application [application of 6 g calcium superphosphate containing 16% P_2O_5 to each pot every 15 days thrice, (+P)]. The amount of P application was determined by the highest concentration of available P loss from bamboo soil (Chen et al., 2011). At the end of the first P application, two water treatments were applied by withholding soil water: well-watered (80% relative soil water content, RSWC) and water-stressed (30% RSWC). The RSWC of each treatment was controlled according to the weight method as described by Xu et al. (2009). In each

treatment, four replicates, each including five standard plants, were used. To reduce systematic errors caused by the possible fluctuations of environmental conditions, all pots were rotated every five days during the experiment. The youngest fully expanded leaves at the same developmental stage were collected for biochemical analyses at the end of the experiment.

2.2. Water status of leaves

The leaves were detached at around 9:00 a.m. and weighed immediately to obtain fresh weight (FW). After, leaves were placed in a beaker containing deionized water at room temperature and reweighed after 12 h to gain turgid weight (TW). Dry weight (DW) was taken by placing leaves in an oven for 24 h at 70 °C. Leaf relative water content (LRWC) was calculated as: LRWC = [(FW − DW)/(TW − DW)] × 100%.

2.3. Gas exchange and chlorophyll a fluorescence measurements

The youngest fully expanded leaves at the same developmental stage were selected to measure gas exchange and Chl *a* fluorescence using a portable analyzer equipped with a fluorometer attachment (LI-6400, LI-COR Inc., USA). The net photosynthetic rate (P_n), stomatal conductance (g_s), intercellular CO_2 concentration (C_i), light-adapted maximum (F_m') and minimum fluorescence (F_o'), and steady-state fluorescence yield (F_s) were measured during the late morning (9:00–11:00 h). After the measurements of the irradiance-adapted parameters, the same leaves were dark-adapted with leaf clips for 40 min. Afterward, the minimum fluorescence yields (F_o) was determined under a weak pulse of modulated light over a 0.8 s, and the maximum fluorescence yields (F_m) and the maximum quantum efficiency of photosystem II (PSII) [F_v/F_m, $(F_m - F_o)/F_m$] were recorded under a saturating pulse of 8000 μmol m^{-2} s^{-1}. During the measurements, leaf temperature, CO_2 concentration in leaf chamber and photosynthetic photon flux density were maintained at 25 °C, 380 ± 5 μmol mol^{-1}, and 800 μmol photons m^{-2} s^{-1}, respectively. Thereafter, the quantum yield of PSII electron transport [Φ_{PSII}, $(F_m' - F_s)/F_m'$] and the efficiency of thermal dissipation [NPQ, $(F_m - F_m')/F_m'$] were calculated.

2.4. Energy flux estimation

The quantum efficiency of photochemical energy dissipation (Φ_{PSII}, $1 - F_s/F_m'$), △pH- and xanthophyll-regulated thermal dissipation (Φ_{NPQ}, $F_s/F_m' - F_s/F_m$), and fluorescence and constitutive thermal dissipation ($\Phi_{f,D}$, F_s/F_m) were calculated as described by Hendrickson et al. (2004) with $\Phi_{PSII} + \Phi_{NPQ} + \Phi_{f,D} = 1$. The flux of energy dissipation in each process (J_{PSII}, J_{NPQ}, and $J_{f,D}$) was calculated by multiplying its respective quantum efficiency by the assumed proportion of absorbed quanta used by PSII reaction centers, irradiance, and leaf absorption coefficient (Harley et al., 1992). The utilization of photons absorbed by the PSII antenna in photosynthetic electron transport and thermal dissipation was then assessed from the quantum efficiency and flux of each process. The rate of electron transport through PSII (J_{PSII}) was determined as described by Harley et al. (1992). The rates of oxygenation (V_o) and carboxylation (V_c) by Rubisco were estimated as described by Miyake and Yokota (2000). Under atmospheric conditions, electron fluxes in the cycles of photosynthetic carbon reduction (J_{PCR}) and photorespiratory carbon oxidation (J_{PCO}) can be expressed as $J_{PCR} = 4 \times V_c$ and $J_{PCO} = 4 \times V_o$, respectively. An alternative electron flux (J_a), caused by electrons that are not used by PCR and PCO cycles in total electron flux driven by PSII was estimated from $J_{PSII} - J_{PCR} - J_{PCO}$. J_a(O_2-dependent) was estimated from the difference between J_a(21% O_2) and J_a(2% O_2), and then J_a(O_2-independent) was estimated from $J_a - J_a$(O_2-dependent) (Zhou et al., 2004).

2.5. Leaf pigment analysis

Fresh leaves (0.3 g) were extracted with 80% acetone in the dark, filtered through a 0.45 μm membrane, and used for the measurements of Chl and xanthophyll cycle pool (A, antheraxanthin; V, violaxanthin; Z, zeaxanthin) using HPLC (Waters 2695 system) as described by Thayer and Björkman (1990). A column of Spherisorb C18 (5 μm, 250 × 4 mm) was used at a flow rate of 1.5 mL min^{-1}. Elution was carried out using acetonitrile/methanol (75: 25, v/v) and methanol/ethyl acetate (70: 30, v/v) as mobile phases A and B, respectively. The elution gradient was started with 100% A for 7 min, increased to 100% B within 2 min, and then maintained for 23 min after 100% B. The column was re-equilibrated with 100% A for 5 min before the next injection. A total of 10 μL of the extract was injected into HPLC, and the pigments were detected through their respective absorbance at 445 nm. The de-epoxidation state (DEPS) of xanthophyll cycle was expressed as the percentage of (0.5A + Z)/(VAZ).

2.6. Purification of cell organelles and antioxidative enzyme activities analysis

Organelles were isolated from fresh leaves using differential and density-gradient centrifugation as described by Mittova et al. (2000) with some modifications. Briefly, leaves (10 g) were chopped using a blender (HR-2826, PHILIPS, China) with 5 vol of medium containing 50 mM HEPES (pH 7.5), 5 mM γ-caproic acid, 0.3% bovine serum albumin, 0.3 M sucrose, 10 mM NaCl, 10 mM β-mercaptoethanol, 5 mM sodium ascorbate, 2 mM EDTA, and 1% polyvinylpyrrolidone. The homogenates were filtered through four layers of gauze. The sediment of the crude chloroplast fraction was obtained via centrifugation at 1000*g* for 5 min at 4 °C, and then purified through 10%, 40%, 70%, and 90% discontinuous Percoll gradient centrifugations at 4700*g* for 15 min. An intact chloroplast layer was obtained between 40% and 70% Percoll fractions. The chloroplast integrity was measured using the ferricyanide method (Song et al., 2009). A total of 1000*g* supernatant was recentrifuged at 12000*g* for 15 min, and the pellet was collected and resuspended in a medium containing 20 mM HEPES-KOH (pH 7.5), 330 mM sorbitol, 10 mM NaCl and 2 mM EDTA. In this isolation procedure, the 12000*g* supernatant was considered to be cytosol fraction. The 12000*g* pellets were fractionated using 25%, 37%, 45%, and 57% sucrose discontinuous gradients at 68000*g* for 3.5 h, and an intact mitochondria layer between 37% and 45% sucrose fractions was collected. The isolated mitochondria integrity was estimated using Cyt *c* method (Song et al., 2009). Finally, these isolated organelles were used for analyses of the following enzymes.

SOD (EC 1.15.1.1) activity was determined by monitoring the inhibition of photochemical reduction of *p*-nitro blue tetrazolium in A_{560} according to Giannopolitis and Ries (1977). Ascorbate peroxidase (APX, EC 1.11.1.11) activity was analyzed by observing the decrease in reduced ascorbate (AsA) in A_{290} (Nakano and Asada, 1981). Monodehydroascorbate reductase (MDHAR, EC 1.6.5.4) activity was assayed by monitoring the decrease in A_{340} due to NADH oxidation (Arrigoni et al., 1981). Dehydroascorbate reductase (DHAR, EC 1.8.5.1) activity was determined following the formation of AsA from oxidized ascorbate (DHA) in A_{265} (Dalton et al., 1986). Glutathione reductase (GR, EC 1.6.4.2) activity was determined by monitoring the decrease in A_{340} caused by NADPH oxidation (Madamanchi and Alscher, 1991).

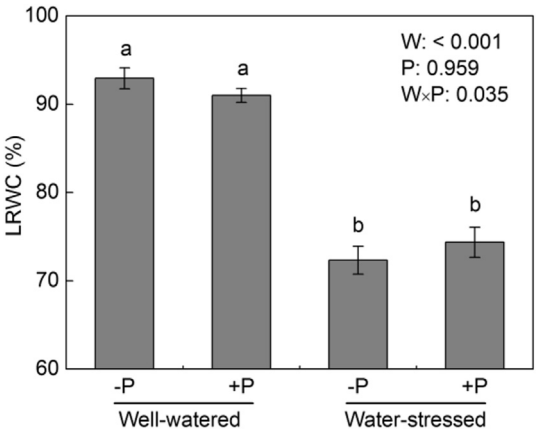

Fig. 1. Leaf relative water content (LRWC) of *F. rufa* plants for non-fertilized (−P) and fertilized (+P) treatments with and without water stress. W, water effect; P, phosphorus effect; W × P, interactive effect of water and phosphorus. Values with different letters are significantly different at $P < 0.05$. Vertical bars show ± S.E.

2.7. Antioxidants determination

The contents of total (tAsA) and reduced (AsA) ascorbate were measured as described by Law et al. (1983). Fresh leaves (0.2 g) were extracted with 5% ice-cold trichloroacetic acid (TCA) and centrifuged at 15000*g* for 15 min at 4 °C. The reactive mixture for tAsA contained supernatant, 150 mM phosphate buffer (pH 7.4, containing 5 mM EDTA), and 10 mM dithiothreitol (DTT). After incubation for 10 min, 0.5% *N*-ethylmaleimide was added to remove excess DTT. AsA was assayed in a similar method as tAsA, except that deionized H_2O was substituted for DTT and *N*-ethylmaleimide. Color was developed in both reactive mixtures following the addition of 10% TCA, 44% orthophosphoric acid, 4% α,α′-bipyridyl, and 3% $FeCl_3$. The mixtures were then incubated at 40 °C for 40 min and quantified at 525 nm. DHA was estimated by subtracting AsA from tAsA.

The contents of total (tGSH) and oxidized (GSSG) glutathione were determined as described by Law et al. (1983). Fresh leaves (0.2 g) were extracted with 6% ice-cold metaphosphoric acid and centrifuged at 12000*g* for 20 min at 4 °C. The reactive mixture for tGSH contained 100 mM phosphate buffer (pH 7.5), 0.6 mM 5,5′-dithiobis-(2-nitrobenzoic acid), 0.2 mM NADPH, 50 U mL^{-1} GR and supernatant. GSSG was assayed in a similar method as tGSH, except that supernatant was pretreated with 2-vinylpyridine at 25 °C for 1 h. The mixtures were quantified at 412 nm. GSH was estimated from the difference between tGSH and GSSG.

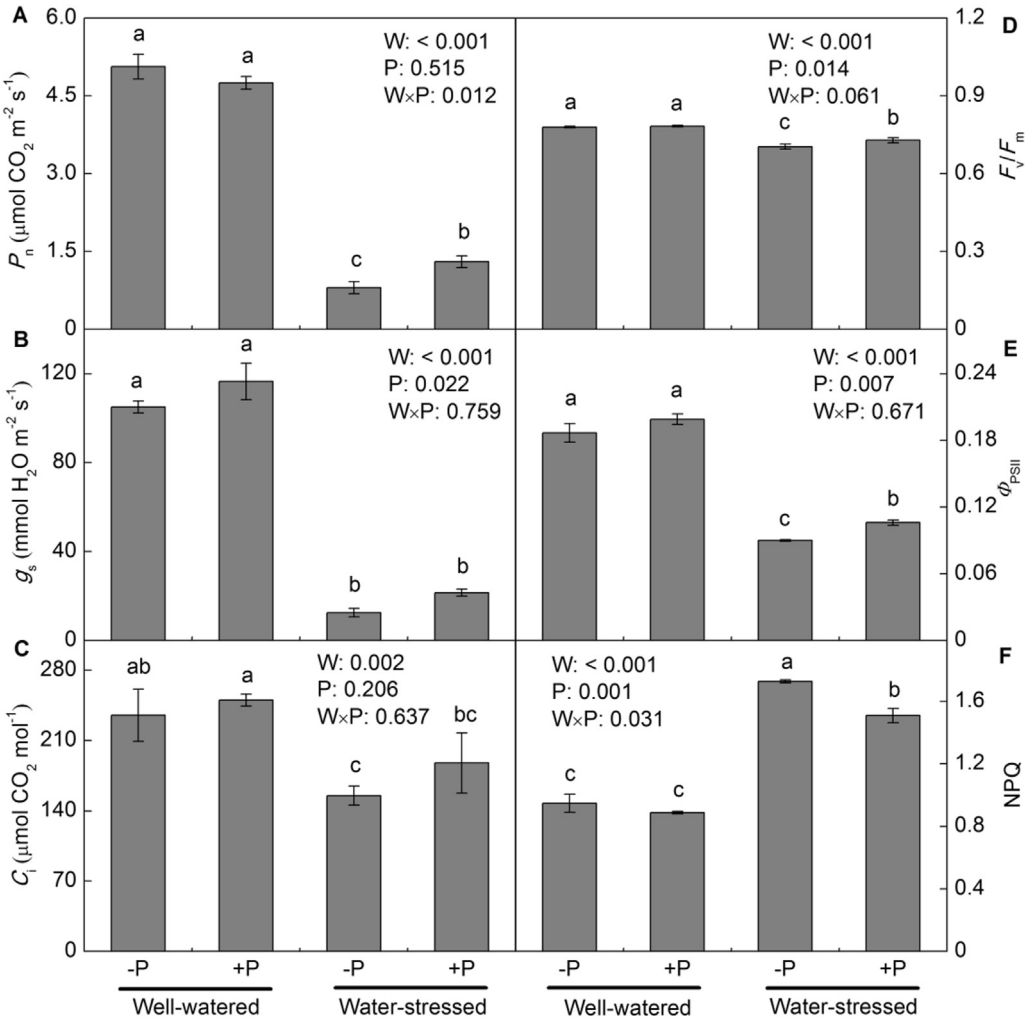

Fig. 2. Gas exchange and chlorophyll *a* fluorescence of *F. rufa* plants for non-fertilized (−P) and fertilized (+P) treatments with and without water stress. W, water effect; P, phosphorus effect; W × P, interactive effect of water and phosphorus. Values with different letters are significantly different at $P < 0.05$. Vertical bars show ± S.E.

2.8. Determination of ROS and lipid peroxidation

The rate of $O_2^{\bullet-}$ production was measured by analyzing the nitrite formation from hydroxylamine according to the method of Elstner and Heupel (1976). Fresh leaves (0.2 g) were homogenized using 65 mM phosphate buffer (pH 7.8) and centrifuged at 5000*g* at 4 °C for 10 min. The incubation mixture contained supernatant, 65 mM phosphate buffer, and 10 mM hydroxylammonium chloride. After incubating at 25 °C for 20 min, the incubation mixture was added with 17 mM sulphanilamide and 7 mM α-naphthylamine, maintained at 25 °C for 20 min, mixed with the same volume of ethyl ether, and then centrifuged at 1500*g* for 5 min. The absorbance of the final incubation mixture was recorded at 530 nm.

H_2O_2 content was measured by monitoring the titanium-peroxide complex at 410 nm, following the method of Patterson et al. (1984). Fresh leaves (0.2 g) were homogenized in ice-cold acetone and centrifuged at 3000*g* for 10 min. The reactive mixture, containing supernatant, titanium reagent (20% $TiCl_4$ in concentrated HCl), and ammonia, was centrifuged at 3000*g* for 10 min. The obtained precipitate was washed five times with acetone, centrifuged at 10000*g* for 5 min, and solubilized with 1 M H_2SO_4.

Lipid peroxidation was estimated by measuring malondialdehyde (MDA) content via thiobarbituric acid (TBA) test at 532 and 600 nm (Zhou et al., 2004). Fresh leaves (0.2 g) were homogenized in 50 mM phosphate buffer (pH 7.8) and centrifuged at 12000*g* for 20 min. Supernatant (1 mL) was mixed with 20% TCA with 2% TBA. The reactive mixture was incubated in a water bath (95 °C, 30 min), rapidly cooled in an ice bath, and then centrifuged at 15000*g* for 10 min. The amount of MDA-TAB complex was calculated using an extinction coefficient of 155 mM^{-1} cm^{-1}.

2.9. Statistical analyses

One- and two-way ANOVA were performed using SAS 9.1 program. One-way ANOVA was used to determined differences among treatments, and Duncan's multiple range test was employed to detect possible differences among means at a 5% probability level. Two-way ANOVA was used to separate the effects of water and P and their interaction. Data were checked for normality and homogeneity of variances and log-transformed to corrected

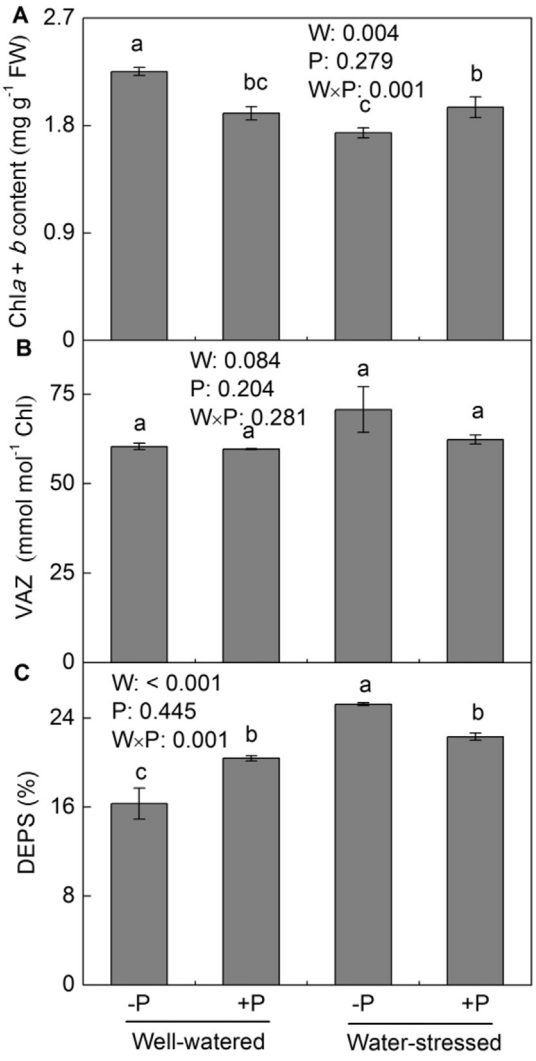

Fig. 3. Contents and de-epoxidation state (DEPS) of xanthophyll cycle pool (VAZ) and chlorophyll *a*+*b* (Chl *a*+*b*) of *F. rufa* plants for non-fertilized (−P) and fertilized (+P) treatments with and without water stress. Violaxanthin (V), antheraxanthin (A), and zeaxanthin (Z). DEPS is calculated as the percentage of (0.5A + Z)/VAZ. W, water effect; P, phosphorus effect; W × P, interactive effect of water and phosphorus. Values with different letters are significantly different at $P < 0.05$. Vertical bars show ± S.E.

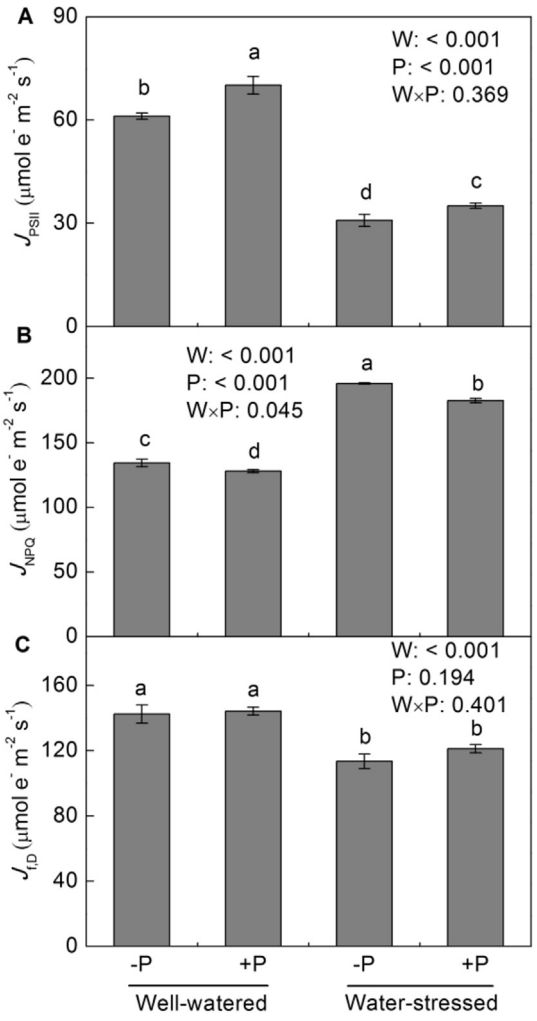

Fig. 4. Energy flux *via* linear electron transport in PSII (J_{PSII}), flux for energy loss *via* △pH- and xanthophyll-regulated thermal dissipation (J_{NPQ}) and *via* fluorescence and constitutive thermal dissipation ($J_{f,D}$) of *F. rufa* plants for non-fertilized (−P) and fertilized (+P) treatments with and without water stress. W, water effect; P, phosphorus effect; W × P, interactive effect of water and phosphorus. Values with different letters are significantly different at $P < 0.05$. Vertical bars show ± S.E.

deviations from these assumptions if necessary.

3. Results

3.1. Leaf relative water content, gas exchange, and Chl a fluorescence

Fig. 1 shows that LRWC in water-stressed plants was lower than that in well-watered ones. Moreover, LRWC was only significantly affected by the interaction of water and P. Regardless of P application, water stress substantially decreased P_n, g_s, C_i, F_v/F_m, and Φ_{PSII} but increased NPQ (Fig. 2). P application had no effects on the above parameters in well-watered plants, whereas it caused significant increases in P_n (61.7%), F_v/F_m (3.4%), and Φ_{PSII} (17.8%), as well as a decrease in NPQ (12.6%) in water-stressed plants. The interactive effects of water and P on P_n and NPQ were significant.

3.2. Pigments

Regardless of P application, water stress did not alter VAZ level (Fig. 3B). A decrease in Chl $a+b$ content and an increase in DEPS ratio were observed in P-unfertilized plants after water stress (Fig. 3A, C). P application had no effect on VAZ level regardless of water availability, whereas it increased the Chl $a+b$ content (12.3%) and decreased the DEPS ratio (11.6%) in water-stressed plants. Furthermore, Chl $a+b$ content and DEPS were significantly affected by the interaction of water and P.

3.3. Energy flux allocation

Regardless of P application, water stress significantly decreased J_{PSII} and $J_{f,D}$ but increased J_{NPQ} (Fig. 4). P application increased J_{PSII} by 14.7% and 13.8% in well-watered and water-stressed plants, respectively, whereas it decreased J_{NPQ} by 4.7% and 6.8% in the corresponding ones (Fig. 4A and B). However, $J_{f,D}$ did not change after P was supplied, irrespective of water availability (Fig. 4C). Moreover, J_{NPQ} was significantly affected by the interaction of water and P.

J_{PCR}, J_{PCO}, $J_a(O_2$-dependent), and $J_a(O_2$-independent) in well-watered plants accounted for approximately 51.2%, 19.9%, 23.7%, and 5.2% of J_{PSII} under P-unfertilized conditions, respectively (Fig. 5). Similarly, these four parameters in well-watered plants accounted for approximately 46.8%, 16.7%, 25.4%, and 11.1% of J_{PSII} under P-fertilized conditions, respectively. Therein, P application significantly increased the proportion of $J_a(O_2$-independent) to J_{PSII} in well-watered plants (Fig. 5D). Moreover, water stress resulted in reduced proportions of J_{PCR} and J_{PCO} to J_{PSII}, as well as increased proportions of $J_a(O_2$-dependent) and $J_a(O_2$-independent) to J_{PSII} regardless of P application. However, the interactive effects of water and P on J_{PCR}, J_{PCO}, $J_a(O_2$-dependent), and $J_a(O_2$-independent) were not significant.

3.4. Antioxidative enzyme activities and antioxidants

Water stress increased the activities of antioxidative enzymes in different organelles (Table 1). In chloroplasts, P application increased SOD activity by 18.8% in well-watered plants, whereas it decreased APX activity by 26.4% in water-stressed plants. In mitochondria, P application increased SOD activity in well-watered plants, whereas it decreased the activities of SOD (15.8%), APX (33.3%), MDHAR (25.7%), and DHAR (32.9%) in water-stressed plants. In cytosol, P application decreased the activities of SOD (9.6%), MDHAR (28.9%), and GR (45.7%) in water-stressed plants. Moreover, DHAR activity in different organelles was consistently higher than MDHAR activity in all treatments. In general, the interactive effects of water and P on these antioxidative enzyme activities were not significant.

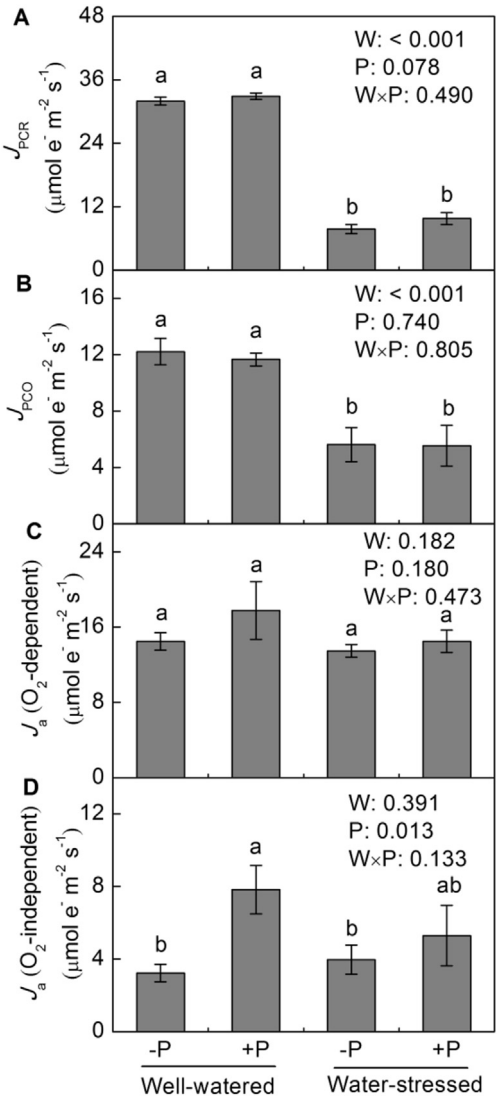

Fig. 5. Electron flux *via* linear electron transport in PSII, including electron flux for photosynthetic carbon reduction (J_{PCR}), electron flux for photorespiratory carbon oxidation (J_{PCO}), O_2-dependent alternative electron flux [$J_a(O_2$-dependent)], and O_2-independent alternative electron flux [$J_a(O_2$-independent)] of *F. rufa* plants for non-fertilized (−P) and fertilized (+P) treatments with and without water stress. W, water effect; P, phosphorus effect; W × P, interactive effect of water and phosphorus. Values with different letters are significantly different at $P < 0.05$. Vertical bars show ± S.E.

Overall, water stress increased the contents of tAsA, AsA, tGSH, and GSH, and decreased the ratios of AsA/DHA and GSH/GSSG under the same P treatment (Fig. 6). P application had no effect on the contents of tAsA and AsA in well-watered plants, whereas it caused significant increases in tAsA (23.2%) and AsA (34.0%) in water-stressed plants (Fig. 6A and B). Regardless of water availability, P application decreased the contents of tGSH and GSH (Fig. 6D and E) and slightly increased the ratios of AsA/DHA and GSH/GSSG (Fig. 6C, F). Moreover, the interactive effects of water and P on tAsA and AsA were significant.

3.5. ROS and lipid peroxidation

Irrespective of P application, water stress increased ROS accumulation, except H_2O_2 content, under P-fertilized conditions,

Table 1
Specific activities of antioxidative enzymes of *F. rufa* plants for non-fertilized (−P) and fertilized (+P) treatments with and without water stress. SOD, superoxide dismutase; APX, ascorbate peroxidase; MDHAR, monodehydroascorbate reductase; DHAR, dehydroascorbate reductase; GR, glutathione reductase. SOD is expressed as U mg^{-1} protein; APX is expressed as μmol mg^{-1} protein min^{-1}; MDHAR, DHAR, and GR are expressed as nmol mg^{-1} protein min^{-1}. F_w, water effect; F_p, phosphorus effect; and $F_{w \times p}$, interactive effect of water and phosphorus. Values followed by the same letter are not significantly different at $P < 0.05$.

Organelle/treatment		SOD	APX	MDHAR	DHAR	GR
Chloroplasts						
Well-watered	−P	3.2 ± 0.1 b	0.41 ± 0.02 c	35.4 ± 3.9 a	59.2 ± 5.7 a	75.8 ± 6.0 ab
	+P	3.8 ± 0.2 a	0.34 ± 0.04 c	36.0 ± 4.8 a	47.6 ± 4.5 a	51.1 ± 8.7 b
Water-stressed	−P	3.8 ± 0.1 a	0.87 ± 0.05 a	35.3 ± 3.0 a	58.3 ± 6.7 a	107.0 ± 18.3 a
	+P	3.6 ± 0.1 a	0.64 ± 0.02 b	33.2 ± 1.8 a	51.0 ± 4.3 a	90.4 ± 3.7 a
$P > F_w$		0.069	<0.001	0.683	0.831	0.011
$P > F_p$		0.073	0.003	0.841	0.117	0.090
$P > F_{w \times p}$		0.004	0.058	0.708	0.699	0.717
Mitochondria						
Well-watered	−P	45.8 ± 1.1 d	0.64 ± 0.02 b	23.4 ± 1.8 c	156.5 ± 13.9 ab	79.0 ± 12.6 ab
	+P	59.7 ± 2.3 c	0.50 ± 0.04 b	18.1 ± 2.1 c	154.7 ± 12.9 ab	65.0 ± 4.6 b
Water-stressed	−P	97.3 ± 7.3 a	0.87 ± 0.07 a	41.6 ± 2.7 a	196.5 ± 18.0 a	100.3 ± 6.0 a
	+P	81.9 ± 3.5 b	0.58 ± 0.04 b	30.9 ± 2.2 b	131.8 ± 16.4 b	93.8 ± 13.9 ab
$P > F_w$		<0.001	0.010	<0.001	0.596	0.038
$P > F_p$		0.863	0.002	0.007	0.063	0.341
$P > F_{w \times p}$		0.009	0.169	0.266	0.075	0.721
Cytosol						
Well-watered	−P	4.4 ± 0.2 bc	0.33 ± 0.02 a	5.2 ± 0.5 c	61.9 ± 8.4 bc	22.3 ± 1.3 b
	+P	4.0 ± 0.1 c	0.32 ± 0.08 a	6.7 ± 0.4 c	57.0 ± 0.5 c	24.1 ± 2.9 b
Water-stressed	−P	5.2 ± 0.1 a	0.53 ± 0.04 a	12.8 ± 0.4 a	87.4 ± 5.6 a	57.1 ± 3.9 a
	+P	4.7 ± 0.1 b	0.48 ± 0.09 a	9.1 ± 0.5 b	77.1 ± 1.3 ab	31.0 ± 1.6 b
$P > F_w$		0.001	0.019	<0.001	0.002	<0.001
$P > F_p$		0.012	0.602	0.047	0.176	0.002
$P > F_{w \times p}$		0.902	0.720	0.001	0.616	0.001

thereby resulting in a high degree of lipid peroxidation, as shown by MDA content (Fig. 7). In well-watered plants, P application increased ROS but had no effect on MDA content. By comparison, P application induced a significant decline in MDA content (23.4%) in water-stressed plants, accompanied by constant $O_2^{\bullet-}$ production and decreased H_2O_2 content. Moreover, the interactive effects of water and P on H_2O_2 content were significant.

4. Discussion

Water status as a regulatory switch for plant response to stresses is often denoted by LRWC in terms of the physiological consequence of cellular dehydration. LRWC can reliably reflect the capacity of plants to re-establish their water balance after undergoing water stress to adapt to or tolerate this stress (Liu et al., 2017b). LRWC of *F. rufa* plants was substantially reduced (*ca.* 25%) after water stress, but it was not affected by P application (Fig. 1), and this result is in line with previous findings in other plants, such as beans and cotton (Garg et al., 2004; Singh et al., 2006; Burman et al., 2009). However, the LRWC decline in response to stress was comparatively less in P-fertilized than unfertilized *F. rufa* plants, indicating that P application can slightly improve plant water status under water stress. This result might be due to the enhanced capability of roots to absorb water from low-water potential soil through relatively rapid growth, increased xylem hydraulic conductivity, and stomata closure (Singh and Sale, 2000; Jones et al., 2005).

Photosynthesis is among the most sensitive physiological processes to water stress. The limitation of P_n in *F. rufa* plants was observed under water stress, as partly due to synchronous decreases in g_s and C_i (Fig. 2B and C), and this condition is because stomatal closure will prevent CO_2 diffusion into mesophyll cells and further inhibit CO_2 assimilation capacity (Gallé et al., 2007; Liu et al., 2017b). Moreover, this result was mainly attributed to impairment in PSII function, as can be further confirmed by the decreases in F_v/F_m and Φ_{PSII} (Fig. 2D and E) as well as Chl degradation (Fig. 3A). Water stress can result in impaired chloroplast photoassimilatory metabolism by reducing inorganic P uptake in the roots and the availability of leaf P_i for the contribution of phosphate translocators to the ratio of P_i/triose phosphate (Hernández and Munné-Bosch, 2015; Simancas et al., 2016); however, P application increased CO_2 assimilation rate in water-stressed plants (Garg et al., 2004; Burman et al., 2009; Sato et al., 2010; Kuwahara et al., 2016). Similarly, after P was supplied, P_n in water-stressed *F. rufa* plants was significantly improved due to PSII repair and Chl synthesis. By contrast, P_n was not affected by P application in well-watered plants because of their continued growth and photoassimilatory export for maintaining P_i reserves in the vacuoles and cytoplasm (dos Santos et al., 2004; Liu et al., 2015a).

However, excess excitation energy will be inevitably caused when inhibition of photosynthetic capacity is not sufficient to utilize the amount of P-based ATP and NADPH. NPQ, an indicator of excitation energy dissipation in PSII antenna, significantly increased in water-stressed *F. rufa* plants (Fig. 2F) and had a strong correlation with DEPS ($r^2 = 0.63$, $P < 0.001$), which is believed to protect the photosynthetic apparatus from photooxidative damage (Gallé et al., 2007). Interestingly, stress-induced increased proportion of NPQ was smaller in P-fertilized than unfertilized plants, accompanied with VAZ and DEPS (Fig. 3B and C), similar to that previously observed in *Phaseolus vulgaris* (dos Santos et al., 2006). The results indicated that after P application, the dissipation of high excitation energy in water-stressed *F. rufa* plants is no longer needed, being associated with i) excessive ATP and NADPH consumed by improved photosynthetic capacity to a certain extent, as proven by increased P_n in this case (Fig. 2A), and ii) thereby accelerating electron transport to other cellular compartments.

Changes in photosynthetic capacity are related to energy and electron transductions. Hence, quantifying the fate of photon energy absorbed by PSII antenna (J_{NPQ}, $J_{f,D}$ and J_{PSII}) is necessary. They are competitive in general; however, an explicit trade-off exists among the three fates of energy (Liu et al., 2017b). In water-stressed *F. rufa* plants, an increase in J_{NPQ} was consistently accompanied by decreases in J_{PSII} and $J_{f,D}$ regardless of P application (Fig. 4), thereby

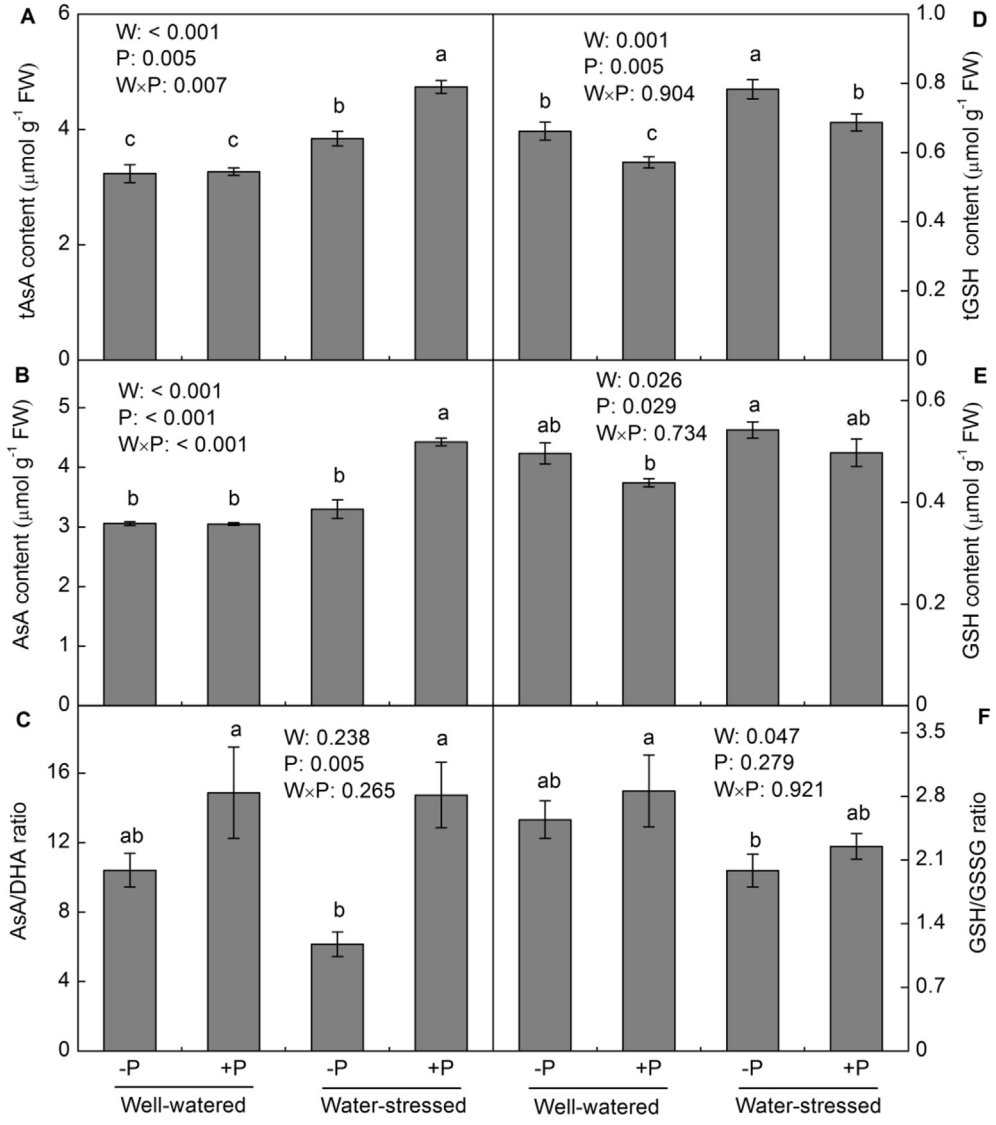

Fig. 6. Antioxidants contents of *F. rufa* plants for non-fertilized (−P) and fertilized (+P) treatments with and without water stress. tAsA, total ascorbate [the sum of reduced (AsA) and oxidized (DHA) ascorbate]; tGSH, total glutathione [the sum of reduced (GSH) and oxidized (GSSG) glutathione]. W, water effect; P, phosphorus effect; W × P, interactive effect of water and phosphorus. Values with different letters are significantly different at $P < 0.05$. Vertical bars show ± S.E.

indicating that VAZ cycle-regulated thermal dissipation is an efficient photoprotective pathway under water stress. However, Zhou et al. (2006) observed that J_{NPQ} was changed or even decreased in *Cucumis sativus* after chill stress. This discrepancy could be attributed to the differences in plant species and stress types. In fact, J_{NPQ} does not include only △pH- and VAZ-dependent thermal dissipation but also triplet quenching, as well as direct O_2 and oxidized-PQ-pool quenching. P application significantly reduced J_{NPQ} and increased J_{PSII} in water-stressed *F. rufa* plants, further suggesting that CO_2 assimilation capacity should be improved by the redistribution of total energy regulated after P application.

The energy utilized by PSII photochemistry can be eventually consumed by CO_2 fixation, photorespiration, and the water−water cycle (Miyake and Yokota, 2001). In water-stressed *F. rufa* plants, a significant decline in J_{PCO} in parallel with J_{PCR} (Fig. 5A and B) indicated that photorespiration is not a plausible protective pathway. By contrast, Guan et al. (2004) reported that photorespiration is effective in protecting the photosynthetic apparatus from oxidative damage in *Vitis vinifera* under water deficit. Moreover, the balance of electron fluxes between J_{PCR} and J_{PCO} was not altered after P was supplied. However, P application may increase leaf P recycling in photorespiration to maintain high CO_2 assimilation capacity in woody species (Ellsworth et al., 2015).

The water−water cycle not only functions to fine-tune ATP/NADPH ratio but also produces thylakoid △pH for enhancing DEPS to dissipate excess excitation energy (Hirotsu et al., 2004). However, its importance in photoprotection is still under debate, particularly in P-deficient plants (Weng et al., 2008; Driever and Baker, 2011). $J_a(O_2$-dependent) that is driven by the water−water cycle was not altered in water-stressed *F. rufa* plants but accounted for a great proportion of J_{PSII} (Fig. 5C), indicating that the water−-water cycle in energy dissipation still cannot be ignored, although its compensatory effect for decreased J_{PCR} has now been restricted. Moreover, $J_a(O_2$-independent), as a candidate for the nitrate assimilation (Miyake and Yokota, 2000), was hardly affected by water stress (Fig. 5D), which is associated with a steady nitrogen metabolism in this case (Liu et al., 2015a). P application enhanced $J_a(O_2$-independent) irrespective of water stress, which explains $J_a(O_2$-independent) may be an alternative electron sink for the cyclic flow around PSI (Miyake, 2010).

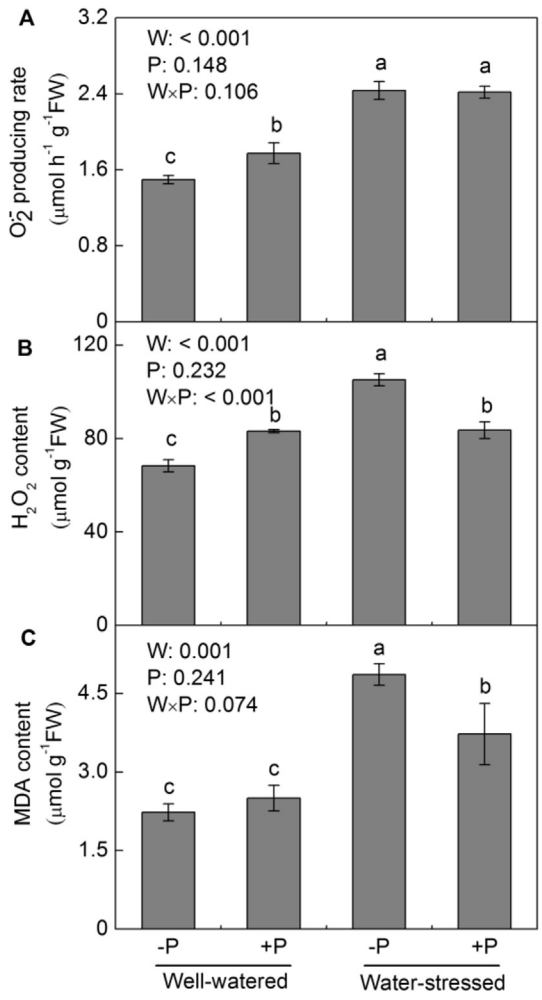

Fig. 7. Producing rate of superoxide anion ($O_2^{\bullet-}$), hydrogen peroxide (H_2O_2) accumulation, and lipid peroxidation (MDA) of *F. rufa* plants for non-fertilized (−P) and fertilized (+P) treatments with and without water stress. W, water effect; P, phosphorus effect; W × P, interactive effect of water and phosphorus. Values with different letters are significantly different at $P < 0.05$. Vertical bars show ± S.E.

Electron transport to O_2 simultaneously carries hazards inherent in ROS formation while causing excessive excitation energy. ROS are continuously generated in different organelles (Hu et al., 2005; Selote and Khanna-Chopra, 2006), particularly chloroplasts and mitochondria because photosynthetic and respiratory electron transport chains are the primary energy-transducing processes associated with ROS generation (Song et al., 2009). ROS play a pivotal role as signal transduction molecules in mediating physiological responses to abiotic stresses in plants (Wujeska et al., 2013); however, its overproduction will cause oxidative damage to cellular structures and disruption of metabolism, thereby leading to cell death. Water stress inevitably induced severe lipid peroxidation of *F. rufa* plants due to ROS accumulation (Fig. 7), and this can be reduced by a coordinated antioxidative system, including upregulated scavenging enzymes in different organelles, particularly mitochondria, and high redox state of antioxidants (Table 1, Fig. 6). P application maintained the normal lipid level in well-watered plants in spite of increased ROS, indicating that redundant ROS may be an important P metabolic signal in this case. By contrast, P application significantly mitigated lipid peroxidation in water-stressed plants with low ROS, particularly H_2O_2, which might be associated with the activation of the H_2O_2-controlling function of AsA independently (Wujeska et al., 2013; Simancas et al., 2016), and meanwhile more electrons (J_{PSII}) transport to photosynthetic CO_2 assimilation (Figs. 2 and 4).

In summary, water stress severely impaired water status, photochemical activity, and cellular membrane, irrespective of P application; however, it increased the capacities of thermal dissipation and antioxidative defense. Furthermore, the role of the water−water cycle in energy dissipation under this stress still could not be ignored because it accounted for a great proportion of J_{PSII}. P application enhanced photochemical activity in water-stressed plants, which was attributed to increased light energy absorbed by increased Chl antenna for the improvement of CO_2 assimilation rate. In this case, the excitation energy dissipated through xanthophyll-regulated heat (J_{NPQ}) was substantially reduced, in which some was transferred as alternative electron sink (J_a). Accordingly, a small quantity of ROS formation, particularly H_2O_2 that was independently controlled by a significant increase in the AsA level alleviated oxidative damage after P application; meanwhile this down-regulated the antioxidative enzymes activities in different organelles. Therefore, only the increased AsA content after P application is able to minimize water stress-induced oxidative damage in *F. rufa* plants, thereby improving the potential functionality of photosynthetic apparatus, which can help them grow well in severe soil water deficit.

Author contributions

CG Liu, YJ Wang and KW Pan designed the experiment. XM Zhou and N Li supplied reagents and materials. CG Liu and YQ Jin performed the experiments. CG Liu analyzed the data and wrote the article. YJ Wang and YQ Jin further revised the manuscript.

Acknowledgements

We thank Ms. Lingling Duan and Mr. Zongping Tang for their help in the field work. We also appreciate Dr. Akash Tariq for valuable comments and grammar revision. This work was financially supported by the National Natural Science Foundation of China (31470621).

References

Adams, W.W., Muller, O., Cohu, C.M., Demmig-Adams, B., 2013. May photoinhibition be a consequence, rather than a cause, of limited plant productivity? Photosynth. Res. 117, 31–44.
Arrigoni, O., Dipierro, S., Borraccino, G., 1981. Ascorbate free radical reductase, a key enzyme of the ascorbic acid system. FEBS Lett. 125, 242–244.
Burman, U., Garg, B., Kathju, S., 2009. Effect of phosphorus application on clusterbean under different intensities of water stress. J. Plant Nutr. 32, 668–680.
Chen, W., Wu, J., Xu, K., Jiang, P., 2011. Soil phosphorus and potential loss in Phyllostachys praecox stands with intensive management. J. Zhejiang A. F. Univ. 28, 687–693.
Cortina, J., Vilagrosa, A., Trubat, R., 2013. The role of nutrients for improving seedling quality in drylands. New For. 44, 719–732.
Dalton, D.A., Russell, S.A., Hanus, F., Pascoe, G.A., Evans, H.J., 1986. Enzymatic reactions of ascorbate and glutathione that prevent peroxide damage in soybean root nodules. Proc. Nati. Acad. Sci. 83, 3811.
Das, K., Roychoudhury, A., 2014. Reactive oxygen species (ROS) and response of antioxidants as ROS-scavengers during environmental stress in plants. Front. Environ. Sci. 2, 1–13.
Divakara, B., Kumar, B.M., Balachandran, P., Kamalam, N., 2001. Bamboo hedgerow systems in Kerala, India: root distribution and competition with trees for phosphorus. Agrofor. Syst. 51, 189–200.
dos Santos, M.G., Ribeiro, R.V., de Oliveira, R.F., Machado, E.C., Pimentel, C., 2006. The role of inorganic phosphate on photosynthesis recovery of common bean after a mild water deficit. Plant Sci. 170, 659–664.
dos Santos, M.G., Ribeiro, R.V., Oliveira, R.F., Pimentel, C., 2004. Gas exchange and yield response to foliar phosphorus application in *Phaseolus vulgaris* L. under drought. Brazil. J. Plant Physiol. 16, 171–179.
Driever, S.M., Baker, N.R., 2011. The water–water cycle in leaves is not a major alternative electron sink for dissipation of excess excitation energy when CO2 assimilation is restricted. Plant Cell Environ. 34, 837–846.
Ellsworth, D.S., Crous, K.Y., Lambers, H., Cooke, J., 2015. Phosphorus recycling in

photorespiration maintains high photosynthetic capacity in woody species. Plant Cell Environ. 38, 1142–1156.
Elstner, E.F., Heupel, A., 1976. Inhibition of nitrite formation from hydroxylammoniumchloride: a simple assay for superoxide dismutase. Anal. Biochem. 70, 616–620.
Eskelinen, A., Harrison, S.P., 2015. Resource colimitation governs plant community responses to altered precipitation. Proc. Nati. Acad. Sci. 112, 13009–13014.
Gallé, A., Haldimann, P., Feller, U., 2007. Photosynthetic performance and water relations in young pubescent oak (*Quercus pubescens*) trees during drought stress and recovery. New Phytol. 174, 799–810.
Gan, H., Jiao, Y., Jia, J., Wang, X., Li, H., Shi, W., Peng, C., Polle, A., Luo, Z., 2016. Phosphorus and nitrogen physiology of two contrasting poplar genotypes when exposed to phosphorus and/or nitrogen starvation. Tree Physiol. 36, 22–38.
Garg, B.K., Burman, U., Kathju, S., 2004. The influence of phosphorus nutrition on the physiological response of moth bean genotypes to drought. J. Plant Nutr. Soil. Sci. 167, 503–508.
Giannopolitis, C.N., Ries, S.K., 1977. Superoxide dismutases: I. Occurrence in higher plants. Plant Physiol. 59, 309–314.
Graciano, C., Guiamét, J.J., Goya, J.F., 2005. Impact of nitrogen and phosphorus fertilization on drought responses in *Eucalyptus grandis* seedlings. For. Ecol. Manag. 212, 40–49.
Graciano, C., Guiamet, J.J., Goya, J.F., 2006. Fertilization and water stress interactions in young *Eucalyptus grandis* plants. Can. J. For. Res. 36, 1028–1034.
Guan, X., Zhao, S., Li, D., Shu, H., 2004. Photoprotective function of photorespiration in several grapevine cultivars under drought stress. Photosynthetica 42, 31–36.
Harley, P.C., Loreto, F., Di Marco, G., Sharkey, T.D., 1992. Theoretical considerations when estimating the mesophyll conductance to CO_2 flux by analysis of the response of photosynthesis to CO_2. Plant Physiol. 98, 1429–1436.
Hendrickson, L., Förster, B., Furbank, R.T., Chow, W.S., 2004. Processes contributing to photoprotection of grapevine leaves illuminated at low temperature. Physiol. Plant. 121, 272–281.
Hernández, I., Munné-Bosch, S., 2015. Linking phosphorus availability with photo-oxidative stress in plants. J. Exp. Bot. 66, 2889–2900.
Hirotsu, N., Makino, A., Ushio, A., Mae, T., 2004. Changes in the thermal dissipation and the electron flow in the water–water cycle in rice grown under conditions of physiologically low temperature. Plant Cell Physiol. 45, 635–644.
Hu, X., Jiang, M., Zhang, A., Lu, J., 2005. Abscisic acid-induced apoplastic H_2O_2 accumulation up-regulates the activities of chloroplastic and cytosolic antioxidant enzymes in maize leaves. Planta 223, 57–68.
Jones, C.A., Jacobsen, J.S., Jon, M., 2005. Response of malt barley to phosphorus fertilization under drought conditions. J. Plant Nutr. 28, 1605–1617.
Kudoyarova, G.R., Dodd, I.C., Veselov, D.S., Rothwell, S.A., Veselov, S.Y., 2015. Common and specific responses to availability of mineral nutrients and water. J. Exp. Bot. 66, 2143–2154.
Kuwahara, F.A., Souza, G.M., Guidorizi, K.A., Costa, C., Meirelles, P.R.D.L., 2016. Phosphorus as a mitigator of the effects of water stress on the growth and photosynthetic capacity of tropical C4 grasses. Acta Sci. Agron. 38, 363–370.
Law, M., Charles, S.A., Halliwell, B., 1983. Glutathione and ascorbic acid in spinach (*Spinacia oleracea*) chloroplasts. The effect of hydrogen peroxide and of Paraquat. Biochem. J. 210, 899–903.
Li, Y., Zhang, Y., Zhang, X., Korpelainen, H., Berninger, F., Li, C., 2013. Effects of elevated CO_2 and temperature on photosynthesis and leaf traits of an understory dwarf bamboo in subalpine forest zone. China. Physiol. Plant. 148, 261–272.
Liu, C., Wang, Q., Jin, Y., Pan, K., Wang, Y., 2017a. Photoprotective and antioxidative mechanisms against oxidative damage in *Fargesia rufa* subjected to drought and salinity. Funct. Plant Biol. 44, 302–311.
Liu, C., Wang, Y., Pan, K., Jin, Y., Li, W., Zhang, L., 2015a. Effects of phosphorus application on photosynthetic carbon and nitrogen metabolism, water use efficiency and growth of dwarf bamboo (*Fargesia rufa*) subjected to water deficit. Plant Physiol. Biochem. 96, 20–28.
Liu, C., Wang, Y., Pan, K., Jin, Y., Liang, J., Li, W., Zhang, L., 2015b. Photosynthetic carbon and nitrogen metabolism and the relationship between their metabolites and lipid peroxidation in dwarf bamboo (*Fargesia rufa* Yi) during drought and subsequent recovery. Trees 29, 1633–1647.
Liu, C., Wang, Y., Pan, K., Wang, Q., Liang, J., Jin, Y., Tariq, A., 2017b. The synergistic responses of different photoprotective pathways in dwarf bamboo (*Fargesia rufa*) to drought and subsequent rewatering. Front. Plant Sci. 8, 489.
Madamanchi, N.R., Alscher, R.G., 1991. Metabolic bases for differences in sensitivity of two pea cultivars to sulfur dioxide. Plant Physiol. 97, 88–93.
Mittova, V., Volokita, M., Guy, M., Tal, M., 2000. Activities of SOD and the ascorbate-glutathione cycle enzymes in subcellular compartments in leaves and roots of the cultivated tomato and its wild salt-tolerant relative *Lycopersicon pennellii*. Physiol. Plant. 110, 42–51.
Miyake, C., 2010. Alternative electron flows (water–water cycle and cyclic electron flow around PSI) in photosynthesis: molecular mechanisms and physiological functions. Plant Cell Physiol. 51, 1951–1963.
Miyake, C., Yokota, A., 2000. Determination of the rate of photoreduction of O_2 in the water-water cycle in watermelon leaves and enhancement of the rate by limitation of photosynthesis. Plant Cell Physiol. 41, 335–343.
Miyake, C., Yokota, A., 2001. Cyclic flow of electrons within PSII in thylakoid membranes. Plant Cell Physiol. 42, 508–515.
Morales, F., Abadía, A., Abadþa, J., 2006. Photoinhibition and Photoprotection under Nutrient Deficiencies, Drought and Salinity. Photoprotection, Photoinhibition, Gene Regulation, and Environment. Springer, pp. 65–85.
Nakano, Y., Asada, K., 1981. Hydrogen peroxide is scavenged by ascorbate-specific peroxidase in spinach chloroplasts. Plant Cell Physiol. 22, 867–880.
Noctor, G., Foyer, C.H., 2016. Intracellular redox compartmentation and ROS-related communication in regulation and signaling. Plant Physiol. 171, 1581–1592.
Patterson, B.D., MacRae, E.A., Ferguson, I.B., 1984. Estimation of hydrogen peroxide in plant extracts using titanium (IV). Anal. Biochem. 139, 487–492.
Sato, A.M., Catuchi, T.A., Ribeiro, R.V., Souza, G.M., 2010. The use of network analysis to uncover homeostatic responses of a drought-tolerant sugarcane cultivar under severe water deficit and phosphorus supply. Acta Physiol. Plant. 32, 1145–1151.
Selote, D.S., Khanna-Chopra, R., 2006. Drought acclimation confers oxidative stress tolerance by inducing co-ordinated antioxidant defense at cellular and subcellular level in leaves of wheat seedlings. Physiol. Plant. 127, 494–506.
Simancas, B., Juvany, M., Cotado, A., Munné-Bosch, S., 2016. Sex-related differences in photoinhibition, photo-oxidative stress and photoprotection in stinging nettle (*Urtica dioica* L.) exposed to drought and nutrient deficiency. J. Photoch. Photobio. B 156, 22–28.
Singh, D.K., Sale, P.W., 2000. Growth and potential conductivity of white clover roots in dry soil with increasing phosphorus supply and defoliation frequency. Agron. J. 92, 868–874.
Singh, S.K., Reddy, V.R., Fleisher, D.H., Timlin, D.J., 2016. Relationship between photosynthetic pigments and chlorophyll fluorescence in soybean under varying phosphorus nutrition at ambient and elevated CO_2. Photosynthetica 55, 1–13.
Singh, V., Pallaghy, C.K., Singh, D., 2006. Phosphorus nutrition and tolerance of cotton to water stress: II. Water relations, free and bound water and leaf expansion rate. Field Crop Res. 96, 199–206.
Suriyagoda, L.D.B., Ryan, M.H., Renton, M., Lambers, H., 2014. Plant responses to limited moisture and phosphorus availability: a meta-analysis. Adv. Agron. 124, 133–200.
Song, X., Wang, Y., Mao, W., Shi, K., Zhou, Y., Nogués, S., Yu, J., 2009. Effects of cucumber mosaic virus infection on electron transport and antioxidant system in chloroplasts and mitochondria of cucumber and tomato leaves. Physiol. Plantarum. 135, 246–257.
Thayer, S.S., Björkman, O., 1990. Leaf Xanthophyll content and composition in sun and shade determined by HPLC. Photosynth Res. 23, 331–343.
Weng, X., Xu, H., Yang, Y., Peng, H., 2008. Water-water cycle involved in dissipation of excess photon energy in phosphorus deficient rice leaves. Biol. Plant. 52, 307–313.
Wujeska, A., Bossinger, G., Tausz, M., 2013. Responses of foliar antioxidative and photoprotective defence systems of trees to drought: a meta-analysis. Tree Physiol. 33, 1018–1029.
Xu, Z., Zhou, G., Shimizu, H., 2009. Are plant growth and photosynthesis limited by pre-drought following rewatering in grass? J. Exp. Bot. 60, 3737–3749.
Yin, C., Pang, X., Chen, K., Gong, R., Xu, G., Wang, X., 2012. The water adaptability of Jatropha curcas is modulated by soil nitrogen availability. Biomass Bioenergy 47, 71–81.
Zhou, Y., Mao, W., Zhang, Y., Huang, L., Hu, W., Yu, J., 2006. Role of thermal dissipation in the photoprotection in cucumber plants after exposure to a chill stress. Photosynthetica 44, 262–267.
Zhou, Y., Yu, J., Huang, L., Nogués, S., 2004. The relationship between CO_2 assimilation, photosynthetic electron transport and water–water cycle in chill-exposed cucumber leaves under low light and subsequent recovery. Plant Cell Environ. 27, 1503–1514.